

Automatic Control of Fluids in Electropneumatic System

Pavel Dimitrov ¹, Mariela Alexandrova ¹

1 - Technical University of Varna, Automation Department, 9010, 1 Studentska Street, Varna, Bulgaria

Corresponding author contact: p.dimitrov@tu-varna.bg

Abstract. This paper presents the design, implementation, and evaluation of an automatic flow control system for electropneumatic applications, incorporating a proportional-integral (PI) control algorithm and an integrated leakage detection mechanism. The proposed system employs a microcontroller-based architecture for real-time pressure monitoring and adaptive valve regulation, using a single pressure sensor and a 4–20 mA transmitter interface. A 5/2 directional valve is utilized for flow routing, while proportional throttle control is achieved through a PWM-driven solenoid valve. The control algorithm dynamically adjusts the output in response to pressure deviations, ensuring stable and accurate regulation within a 0–6 bar range. An automated leak detection logic is embedded to identify abnormal air losses by monitoring persistent high output signals and deviation errors beyond a predefined threshold. Experimental results demonstrate that the system achieves rapid stabilization with minimal steady-state error, maintaining pressure within $\pm 2\%$ of the desired setpoint. Furthermore, the leakage detection functionality effectively isolates fault conditions, enhancing operational safety and energy efficiency. The overall performance validates the practicality of the proposed design as a cost-effective and intelligent solution for industrial pneumatic automation.

Keywords: Electropneumatic systems, PI control, fluid flow regulation, leakage detection, microcontroller-based automation, proportional valve control, adaptive control.

1 Introduction

Electropneumatic systems are a fundamental component of modern industrial automation, where compressed air serves as the primary power source and is controlled via electrical signals. Due to their simplicity, affordability, and durability, these systems are widely used in manufacturing, robotics, and process automation (Lin et al., 2019). Despite these advantages, their operational efficiency can be significantly affected by several limitations, including air leakages, nonlinear flow characteristics, and time-dependent behavior, which collectively complicate precise flow regulation (Rohilla & Singh, 2016).

Among the most persistent challenges, air leakage is particularly detrimental. Undetected or unaddressed leaks can result in substantial compressed air losses, leading to increased energy consumption and higher operational costs (Boyko & Weber, 2024; *Journal of Cleaner Production*, 2020). In addition to economic consequences, leakages compromise system performance by reducing pressure stability, delaying actuator responses, and diminishing overall reliability (Yu, Li, & Tan, 2023). Therefore, developing effective leakage detection and control mechanisms is essential to maintain optimal efficiency in electropneumatic operations (*Procedia CIRP*, 2024).

Another significant challenge arises from the nonlinear behavior of pneumatic components, such as valves and actuators. Conventional control strategies, particularly proportional–integral–derivative (PID) controllers, often exhibit limited performance under conditions such as hysteresis, load variations, and system delays (Rohilla & Singh, 2016). To address these issues, researchers have proposed advanced control algorithms, including adaptive control, fuzzy logic systems, and model predictive control (MPC), which offer improved precision and robustness under variable operating conditions (Lin et al., 2019; Rohilla & Singh, 2016).

Recent advances in intelligent sensors and Internet of Things (IoT) technologies have provided additional solutions to these long-standing problems. Real-time data acquisition and predictive analytics enable automatic fault detection and optimized airflow management, facilitating the transition toward

Industry 4.0-compliant pneumatic networks (*Procedia CIRP*, 2024). These innovations have demonstrated significant potential in enhancing system reliability, reducing energy waste, and promoting sustainable operation (Boyko & Weber, 2024; *Journal of Cleaner Production*, 2020).

Although electropneumatic systems remain integral to industrial automation, challenges related to leakage, nonlinearity, and energy inefficiency persist. The development of automatic flow control and intelligent monitoring systems represents a crucial pathway to achieving higher accuracy, improved energy efficiency, and operational stability in pneumatic automation (Lin et al., 2019; Rohilla & Singh, 2016; Boyko & Weber, 2024; Yu et al., 2023; *Journal of Cleaner Production*, 2020; *Procedia CIRP*, 2024).

2 Problem statement

Although significant progress has been made in control and monitoring technologies, electropneumatic systems still present operational challenges related to energy efficiency, dynamic performance, and monitoring capabilities. Current methods do not sufficiently account for the combined effects of air leakage, nonlinear actuator and valve behavior, and energy losses associated with high supply pressures or limited exhaust and expansion energy recovery. In addition, the practical integration of intelligent monitoring and predictive control into industrial environments remains limited, creating opportunities for further enhancement. The research problem is therefore to develop a unified approach for controlling and monitoring electropneumatic systems that effectively reduces leakage, improves energy utilization, and incorporates real-time intelligent monitoring, while maintaining high accuracy and operational stability.

3 Theoretical analysis

This section outlines the mathematical modeling of a double-acting electropneumatic cylinder system, establishing a formal basis for simulation, analysis, and subsequent control design. The model captures the coupled dynamics of air flow, chamber pressure evolution, and piston motion under nonlinear actuator behavior.

A typical electropneumatic actuator comprises a directional valve regulating airflow into and out of cylinder chambers, a piston with associated mechanical motion, and connecting pneumatic lines. Flow through the valve orifices is often represented by a non-linear orifice equation that depends on the valve opening (spool position), supply pressure, and chamber pressure. The resultant mass flow induces pressure changes in the chambers, while the piston motion responds to the net force generated by the pressure difference, minus friction and external load forces. The state of the system is described by:

$$X = [x, v, P_A, P_B]^T, \quad (1)$$

where x denotes the piston rod position (m), $v = \dot{x}$ its velocity (m/s), and P_A, P_B the pressures in chambers A and B (Pa). The governing equations are formed by combining three subsystems.

3.1 Mechanical dynamics

$$m\ddot{x} = A_A P_A - A_B P_B - F_f(v) - F_{\text{load}}, \quad (2)$$

where m is the moving mass, A_A and A_B are effective piston areas facing chambers A and B, $F_f(v)$ is the friction force (e.g., Coulomb, viscous, or more complex models), and F_{load} is the external load force. This form follows classical actuator modeling in the literature (Sorli, Gastaldi, Codina, & de las Heras, 1999).

3.2 Chamber pressure dynamics

$$\dot{P}_i = \frac{\beta}{V_i(x)} (Q_i - A_i \dot{x}), i \in A, B, \quad (3)$$

where β is the effective bulk modulus of air (or appropriate thermodynamic modulus), $V_i(x)$ the instantaneous chamber volume (e.g., $V_A = V_{A0} + A_A x$, $V_B = V_{B0} + A_B (S - x)$ with stroke S and initial dead volumes V_{A0}, V_{B0}), and Q_i the control mass (or volumetric) flows supplied or exhausted. This formulation is widely adopted in dynamic pneumatic actuator modeling (Ilchmann, Sawodny, & Trenn, 2005).

3.3. Flow subsystem

The mass flow rate through the valve orifice(s), \dot{m}_i , is often described by a nonlinear orifice equation that depends on valve spool displacement (effective area), supply pressure, chamber pressure, and gas properties (e.g., density, compressibility). This introduces strong nonlinearity into the pressure dynamics subsystem, accounting for compressibility, flow choke, and transient behavior typical for pneumatic valves. Such modeling practice is consistent with modern electropneumatic simulation studies (Iliev & Hristov, 2023). Combining these subsystems yields a set of coupled nonlinear ordinary differential equations:

$$\begin{aligned} \ddot{x} &= f_1(x, \dot{x}, P_A, P_B), \\ \dot{P}_A &= f_2(x, \dot{x}, P_A, Q_A), \\ \dot{P}_B &= f_3(x, \dot{x}, P_B, Q_B). \end{aligned} \quad (4)$$

This ODE-based model provides a detailed representation of the actuator's dynamic behavior, allowing simulation of displacement, velocity, and chamber pressure trajectories under arbitrary control flows Q_A, Q_B , or valve commands.

Such models form the analytical foundation for simulation-driven design and control of pneumatic actuation systems. For example, Sorli et al. (1999) presented a double-acting actuator model incorporating both isothermal and adiabatic air transformations, while Nikitin and Levchenko (2024) extended the framework for single-acting cylinders adaptable to double-acting configurations. Overall, this theoretical investigation establishes a robust analytical foundation for further studies, including control design, leakage analysis, energy-efficiency optimization, and real-time monitoring of electropneumatic systems.

4 Modeling and simulation

Based on the theoretical investigation and the mathematical modeling presented in the previous section, a MATLAB model of a double-acting pneumatic cylinder has been developed (Fig. 1) to simulate the dynamic behavior of a physical actuator with a 500 mm stroke, a 25 mm piston rod diameter, and a 100 mm cylinder bore.

The model represents physical interactions governing system dynamics, with state variables describing piston position, velocity, and the pressures in both chambers (Fig. 2), while the piston motion is constrained to remain within the actual stroke length. Chamber volumes are updated continuously as a function of piston displacement, reflecting air compressibility and incorporating minimum-volume limits to prevent numerical singularities during integration. Friction is represented through a Coulomb friction model that adjusts according to motion direction and stabilizes near zero velocity to improve solver robustness. The mechanical response is determined by the net force acting on the piston, which accounts for the pressure differential between chambers, frictional effects, and external loading conditions. Pressure evolution is computed from the interaction between input mass flow rates and volume variations caused by piston motion, enabling a realistic depiction of compression and expansion processes in pneumatic actuation. Saturation constraints are introduced to prevent the occurrence of nonphysical negative pressures. The model also determines the required inlet flow to achieve a prescribed piston velocity and

employs MATLAB's ODE45 solver to simulate the system response over time, yielding time-dependent trajectories for position, velocity, and chamber pressures.

```

function dx = doubleActingPneumatic(~, x, u, p)
  xpos = x(1);
  v = x(2);
  PA = x(3);
  PB = x(4);

  %% Clamp position inside stroke
  xpos = min(max(xpos,0), p.stroke);

  %% Chamber volumes
  VA = max(p.VA0 + p.A_A * xpos, 1e-8);
  VB = max(p.VB0 + p.A_B * (p.stroke - xpos), 1e-8);

  %% Coulomb friction
  if abs(v) < 1e-4
    Ff = 0;
  else
    Ff = p.friction * sign(v);
  end

  %% Mechanical dynamics
  F = p.A_A*PA - p.A_B*PB - Ff - p.load;
  a = F / p.mass;

  %% Pressure dynamics
  dPA = p.beta/VA * (u(1) - p.A_A*v);
  dPB = p.beta/VB * (u(2) + p.A_B*v);

  %% Prevent negative pressures
  dPA = max(dPA, -PA/0.01);
  dPB = max(dPB, -PB/0.01);
  dx = [v; a; dPA; dPB];
end

%% Cylinder geometry & parameters
stroke = 0.5; d_piston = 0.025; d_bore = 0.100;
A_A = pi*d_bore^2/4; A_B = A_A - pi*d_piston^2/4;

params.A_A = A_A; params.A_B = A_B; params.mass = 1.0;
P0 = 1e5; params.beta = 1.4*P0;
params.VA0 = A_A*0.01; params.VB0 = A_B*0.01;
params.stroke = stroke; params.friction = 5; params.load = 0;

%% Initial conditions and desired flow
x0 = [0;0;P0;P0];
v_desired = stroke/10; % 10 s full stroke
Q_required = A_A * v_desired; % m^3/s
u = [Q_required; 0]; % fill chamber A, exhaust B
fprintf("Required flow = %.3e m^3/s\n", Q_required);

%% Solve ODE
odefun = @(t,x) doubleActingPneumatic(t,x,u,params);
[t,X] = ode45(odefun,[0 10],x0);

%% Plots
figure('Color','w','Name','Pneumatic Cylinder 10s Full Stroke');
subplot(3,1,1); plot(t,X(:,1),'LineWidth',1.5); ylabel('Position (m)'); grid on;
on; ylim([0 stroke]);
subplot(3,1,2); plot(t,X(:,2),'LineWidth',1.5); ylabel('Velocity (m/s)'); grid on;
on;
subplot(3,1,3); plot(t,X(:,3)/1e3,'r','LineWidth',1.5); hold on;
plot(t,X(:,4)/1e3,'b','LineWidth',1.5); ylabel('Pressure (kPa)'); xlabel('Time (s)');
legend('P_A','P_B'); grid on;

%% Cylinder dynamics
function dx = doubleActingPneumatic(~, x, u, p)
  q = x(1); v = x(2); PA = x(3); PB = x(4);
  VA = p.VA0 + p.A_A*q; VB = p.VB0 + p.A_B*(p.stroke - q);
  Ff = p.friction*sign(v+1e-6);
  a = (p.A_A*PA - p.A_B*PB - Ff - p.load)/p.mass;
  dPA = p.beta/VA*(u(1) - p.A_A*v);
  dPB = p.beta/VB*(u(2) + p.A_B*v);
  dx = [v; a; dPA; dPB];
end

```

Fig. 1. Model of a double-acting pneumatic cylinder

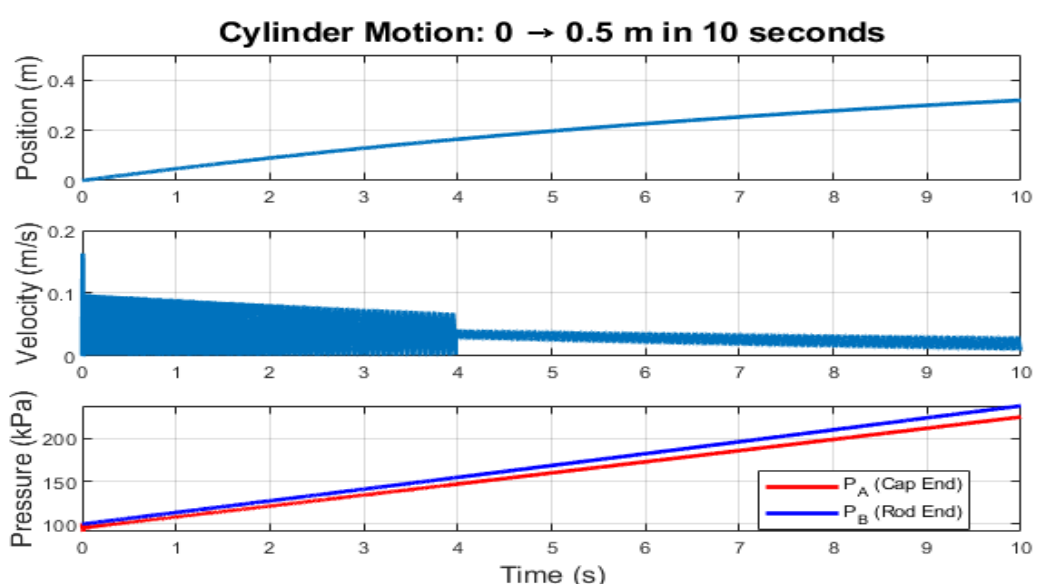


Fig. 2. Piston position, velocity, and the pressures in chambers A and B

5 Control system design

The proposed control system was developed to achieve accurate and reliable regulation of fluid flow and pressure within an electropneumatic actuator using a microcontroller-based architecture. The design integrates analog signal conditioning, closed-loop PI control, adaptive settings, leakage diagnostics, and bidirectional actuation within a unified control framework. The objective of the system is to maintain the desired process pressure under varying load conditions while simultaneously detecting and mitigating operational anomalies such as leakages or directional valve malfunctions.

5.1 System design

The sensing subsystem employs a single industrial-grade pressure transducer with a standard 4–20 mA current output signal, which is converted to a corresponding 1–5 V potential through a $500\ \Omega$ precision shunt resistor. This configuration ensures compatibility with the analog-to-digital converter (ADC) of the control microcontroller and provides high-fidelity pressure feedback. The acquired voltage signal is processed and linearly mapped to the actual pressure range of 0–10 bar, representing the process variable (PV). The operator-defined reference or setpoint (SP) is established using a potentiometer that generates a 0–5 V signal proportional to the target pressure range of 0–6 bar. Both PV and SP values are normalized into percentage units to maintain computational uniformity across different pressure scales and to simplify the controller tuning process. Figure 3 illustrates how each peripheral is mapped to the respective analog and digital ports of the microcontroller.

```

// Single pressure sensor (4–20 mA via 500Ω shunt)
#define PIN_PV      A0    // Only ONE pressure sensor

// Setpoint potentiometer
#define PIN_SP_POT  A1    // 0–5 V → 0–6 bar

// Output control
#define PIN_OUTPUT   3     // PWM output to proportional throttle valve

// 5/2 directional valve solenoids (for direction only)
#define PIN_SOL_A   8     // Solenoid for direction A
#define PIN_SOL_B   9     // Solenoid for direction B

// Direction selector switches (latching)
#define PIN_SW_A    6     // Switch for direction A
#define PIN_SW_B    7     // Switch for direction B

const float SHUNT_RESISTOR = 500.0;    // Ω <<< UPDATED TO 500 OHM
const float VREF           = 5.0;      // ADC reference voltage

const float I_MIN_mA = 4.0;
const float I_MAX_mA = 20.0;

const float P_SENSOR_MAX_BAR = 10.0; // Sensor range 0–10 bar
const float PROCESS_MAX_BAR  = 6.0;  // Controlled process range 0–6 bar

```

Fig. 3. I/O Configuration

The control algorithm is implemented using a digital PI controller based on the PID_v1 library, which executes a continuous feedback loop. The control output, expressed as a duty cycle percentage, is transmitted as a pulse-width modulated (PWM) signal to drive a proportional throttle valve. The PWM output modulates the valve aperture, thus regulating the airflow and maintaining the desired pressure within the pneumatic chamber. To enhance adaptability and dynamic response, a dual-mode tuning strategy is employed (Fig. 4): a conservative gain configuration ($K_p = 1.0$, $K_i = 0.2$, $K_d = 0.0$) is applied during steady-state operation to ensure stability and reduce overshoot, while an aggressive gain set ($K_p = 2.0$, $K_i = 0.5$, $K_d = 0.0$) is utilized during large deviations to improve transient performance. This adaptive switching mechanism allows the system to balance responsiveness and precision under varying process dynamics and nonlinearities inherent to pneumatic systems.

```

double PV_bar;           // Measured pressure in bar
double SP_bar;           // Setpoint in bar

double Input;             // PV in %
double Setpoint;          // SP in %
double Output;            // Controller output in %

double aggKp = 2.0, aggKi = 0.5, aggKd = 0.0;
double consKp = 1.0, consKi = 0.2, consKd = 0.0;

PID myPID(&Input, &Output, &Setpoint, consKp, consKi, consKd, DIRECT);
  
```

```

// 4) Adaptive tuning
double gap = fabs(Setpoint - Input);
if (gap < 5.0) {
  myPID.SetTunings(consKp, consKi, consKd);
} else {
  myPID.SetTunings(aggKp, aggKi, aggKd);
}

// 5) PID execution
if (!leakAlarm) {
  myPID.Compute();
} else {
  Output = 0.0;
}
  
```

Fig. 4. PI Configuration and adaptive settings

Directional control is achieved through a 5/2 solenoid valve actuated by two digital output channels corresponding to forward and reverse motion. The selection of actuation direction is determined by the state of two external switches, each associated with one solenoid. A mutual interlocking software logic ensures that both solenoids cannot be simultaneously energized, thereby preventing valve overlap and potential mechanical damage. This arrangement provides safe, deterministic switching between actuation directions and contributes to the overall robustness of the system.

An integrated leakage detection mechanism (Fig. 5) enhances system reliability and energy efficiency by continuously monitoring control output behavior relative to the pressure response. Leakage conditions are inferred when the controller output remains above a defined threshold of 90% while the pressure error exceeds 0.5 bar for more than 2.5 seconds. Under such circumstances, the controller interprets the condition as an abnormal loss of pressure integrity, indicating a potential leak or actuator malfunction. The system then automatically deactivates the control output and isolates the pneumatic supply to prevent further energy loss or unsafe operation. A visual and serial notification is issued to alert the operator, and system reset can be initiated through a serial “CLR” command once maintenance or inspection is completed. This automated fault management procedure eliminates the need for continuous human supervision and contributes to predictive maintenance within pneumatic automation networks.

```

void handleLeakLogic() {
  
```

```

  if (leakAlarm) {
    Output = 0.0;
    return;
  }

  if (SP_bar <= MIN_SP_FOR_LEAK_BAR) {
    leakTimerStart = 0;
    return;
  }

  double error_bar = SP_bar - PV_bar;

  bool conditionNow =
    (Output > HIGH_OUT_THRESHOLD) &&
    (error_bar > MIN_ERR_FOR_LEAK_BAR);

  if (conditionNow) {
    if (leakTimerStart == 0) {
      leakTimerStart = millis();
    } else {
      if (millis() - leakTimerStart >= LEAK_TIME_MS) {
        leakAlarm = true;
        if (!leakMessageSent) {
          Serial.println("!!! LEAK DETECTED -> SYSTEM SHUTDOWN");
          leakMessageSent = true;
        }
      }
    }
  } else {
    leakTimerStart = 0;
  }
}
  
```

Fig. 5. Leakage detection logic

Real-time monitoring and data acquisition are facilitated through a serial communication interface that transmits key parameters—such as process pressure, setpoint, control effort, solenoid status, and leakage state—to a connected visualization platform. The data stream can be interpreted by the Arduino Serial Plotter or logged for subsequent analysis. This functionality supports both operational monitoring and performance evaluation during system testing and calibration phases.

5.2 Results

The effectiveness of the developed electropneumatic flow control system was validated through a series of experimental tests under both normal and leakage conditions. The corresponding system responses, visualized via the Arduino Serial Plotter, are presented in Figures 6 and 7. These plots show the behavior of the process variable (PV), controller output (OUT), and setpoint (SP) over time, illustrating the transient and steady-state characteristics of the control system.

Under normal operating conditions (Fig. 6), the system demonstrates a rapid pressure rise immediately after the control signal activation, achieving approximately 95–100% of the target setpoint within 2–3 seconds. The rise time (Tr) is estimated to be around 2.1 s, while the settling time (Ts) is observed to be approximately 6–8 s, indicating a fast and stable response. A moderate overshoot of about 10–12% is recorded, followed by gradual attenuation of oscillations as the controller output stabilizes near its steady-state value. The steady-state error remains below 2%, confirming that the implemented PID parameters provide accurate and robust pressure regulation. The adaptive tuning logic, which alternates between aggressive and conservative gain sets, effectively minimizes sustained oscillations while maintaining responsiveness to setpoint variations. These characteristics confirm that the control algorithm successfully balances stability and agility in response to system disturbances and nonlinear valve dynamics.

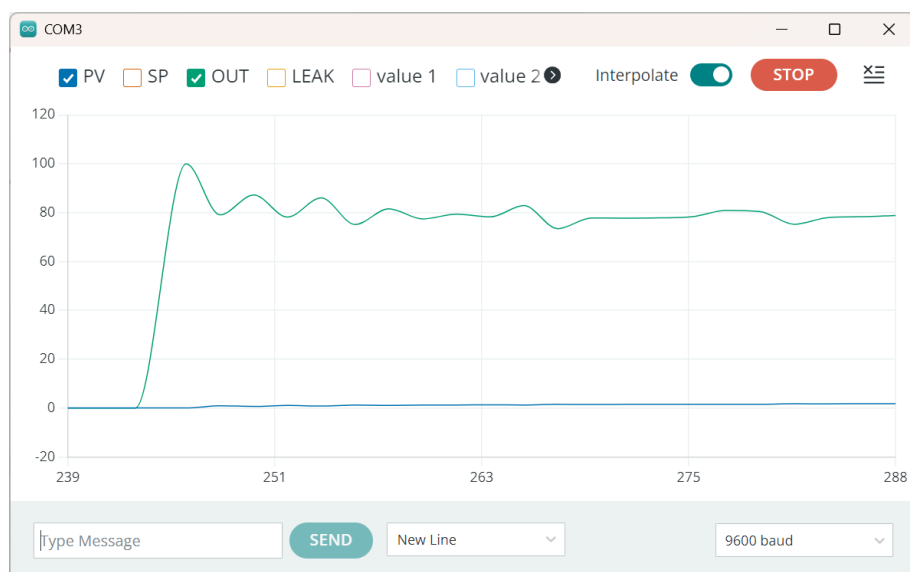


Fig. 6. PI Control

In contrast, the response obtained under simulated leakage conditions (Fig. 7) reveals a distinct deviation from normal behavior. Following setpoint activation, the controller output rapidly saturates to 100%, attempting to compensate for the continuous pressure drop. However, the PV fails to reach the expected setpoint, and the persistent deviation exceeding 0.5 bar over a period longer than 2.5 seconds triggers the built-in leak detection logic. Upon detection, the system automatically disables the actuator outputs, as evidenced by the abrupt drop in the OUT signal to zero. This behavior validates the reliability of the leakage detection algorithm and the robustness of the safety interlock mechanism, which effectively isolates the fault condition to prevent energy losses and potential mechanical damage.



Fig. 7. Leakage detection system response

Quantitatively, the control system exhibits a steady-state precision of $\pm 2\%$, rise time below 3 seconds, and total response settling within 8 seconds, which are within acceptable industrial performance ranges for low-pressure electropneumatic systems. The automated leak response time of approximately 2.5–3 seconds demonstrates efficient fault recognition and corrective action without operator intervention. Overall, these results confirm that the developed control system achieves the intended objectives of maintaining pressure stability, optimizing energy use, and ensuring operational safety. The integration of adaptive PID control with embedded diagnostic logic provides a reliable, autonomous solution suitable for modern Industry 4.0 pneumatic automation applications.

6 Conclusion

The developed automatic control system for fluid flow regulation in electropneumatic system successfully demonstrates a balance between precision, reliability, and energy efficiency. The adaptive PID-based control scheme proved effective in stabilizing pressure output across varying setpoints and operational conditions, achieving fast transient response and minimal overshoot. This outcome confirms that a microcontroller-based platform, when properly tuned, can deliver performance comparable to more complex control architectures while maintaining low implementation cost and computational simplicity.

The integrated leakage detection module further enhances system dependability by continuously assessing control output and process error to identify abnormal pneumatic losses. Experimental testing verified that the mechanism can autonomously detect and respond to leakage conditions within approximately three seconds, automatically isolating the fault to prevent excessive energy waste and equipment stress. This feature aligns with sustainable energy management principles, addressing one of the most persistent challenges in pneumatic automation.

In addition, the system's modular structure and real-time monitoring capability make it suitable for future integration into intelligent manufacturing frameworks. The ability to visualize control behavior through serial data acquisition provides a foundation for data-driven maintenance and diagnostic strategies. Future developments could include extending the control logic with model predictive or fuzzy adaptive algorithms and incorporating IoT-based connectivity for cloud monitoring and predictive analytics. Overall, the presented work validates that effective automatic flow control in electropneumatic systems can be achieved through compact, intelligent, and adaptive embedded solutions.

References

Lin, Z., Wei, Q., Ji, R., Huang, X., Yuan, Y., & Zhao, Z. (2019). An electro-pneumatic force tracking system using fuzzy logic-based volume flow control. *Energies*, 12(20), 4011. <https://doi.org/10.3390/en12204011>

Rohilla, P., & Singh, A. P. (2016). To control nonlinear pneumatic system using fuzzy logic controller. *International Journal of Engineering Research and Technology (IJERT)*, 5(4). <https://doi.org/10.17577/IJERTV5IS040777>

Boyko, V., & Weber, J. (2024). Energy efficiency of pneumatic actuating systems with pressure-based air supply cut-off. *Actuators*, 13(1), 44. <https://doi.org/10.3390/act13010044>

Yu, Q., Li, F., & Tan, X. (2023). Influence analysis and performance optimization of a pneumatic actuator exhaust utilization system. *Strojniški Vestnik – Journal of Mechanical Engineering*, 69(3–4), 119–134. <https://doi.org/10.5545/sv-jme.2022.266>

Energy optimization of pneumatic actuating systems using expansion energy and exhaust recycling. (2020). *Journal of Cleaner Production*, 254, 119983. <https://doi.org/10.1016/j.jclepro.2020.119983>

Pneumatic control for sustainable compressed air systems: Multi-criteria optimisation for energy-efficient production. (2024). *Procedia CIRP*, 122, 247–252. <https://doi.org/10.1016/j.procir.2024.01.035>

Sorli, M., Gastaldi, L., Codina, E., & de las Heras, S. (1999). Dynamic analysis of pneumatic actuators. *Simulation Practice and Theory*, 7(5), 589–602. [https://doi.org/10.1016/S0928-4869\(99\)00012-9](https://doi.org/10.1016/S0928-4869(99)00012-9)

Ilchmann, A., Sawodny, O., & Trenn, S. (2005). Pneumatic cylinders: Modelling and feedback force control. Preprint IST 05/0502.

Iliev, G., & Hristov, H. (2023). Modeling and simulation of an electropneumatic positioning system including the length of pneumatic lines. In *Environmental. Technology. Resources. Proceedings of the International Scientific and Practical Conference*.

Nikitin, A. A., & Levchenko, O. (2024). Position control systems with friction compensation for servo pneumatic actuators. *Mechanics and Advanced Technologies*, 8(4).